

1  **$\delta^{15}\text{N}$  in deployed macroalgae as a tool to monitor nutrient input driven by tourism**  
2 **activities in Mediterranean islands**

3

4 Geraldina Signa<sup>1</sup>, Cristina Andolina<sup>2</sup>, Agostino Tomasello<sup>2</sup>, Antonio Mazzola<sup>1,2</sup>, Salvatrice  
5 Vizzini<sup>1,2</sup>

6

7 **Affiliation**

8 <sup>1</sup>CoNISMa, Consorzio Nazionale Interuniversitario per le Scienze del Mare, Rome, Italy

9 <sup>2</sup>DISTEM, Dipartimento di Scienze della Terra e del Mare, Università degli Studi di Palermo,

10 PA, Italy

11

12 corresponding author: cristina.andolina01@unipa.it

13

14 **Abstract**

15 Mediterranean Sea is among the world's leading tourist destinations; however, the sharp increase  
16 in tourists during the high season may affect coastal seawater. The main aim of this study was to  
17 evaluate the occurrence and temporal variation of anthropogenic nutrients in coastal seawater in  
18 relation to tourist flows in three Mediterranean islands (Cyprus, Sicily and Rhodes), through  
19 short-term macroalgae deployments, coupled with  $\delta^{15}\text{N}$  analysis and GIS mapping. In all islands,  
20 an overall increase in macroalgae  $\delta^{15}\text{N}$  occurred over the deployment carried out in August in the  
21 tourist sites, suggesting the presence of anthropogenic nutrients. Decreasing  $\delta^{15}\text{N}$  values  
22 occurred at increasing distance from the coastline in two out of the three islands (Cyprus and  
23 Sicily). This study revealed the usefulness of the approach used in the assessment of tourism  
24 impact in terms of trophic enrichment and its potential to support competent authorities for the  
25 development of sustainable coastal management plans.

26

27 **Keywords**

28 biomonitoring, indicators, stable isotopes, eutrophication, GIS, *Cystoseira*

29

## 30 **1 Introduction**

31 Mass tourism is a rather recent phenomenon that is leading to considerably high density of  
32 visitors within restricted spaces and periods. Tourism income has greatly increased in recent  
33 years bringing economic benefits to many countries, but there are substantial environmental  
34 threats and costs associated with it (Davenport and Davenport, 2006). Nevertheless, the overall  
35 understanding of the interaction between tourism and environment, especially in marine and  
36 coastal areas is quite poor and fragmented. An example is represented by beaches, as they  
37 provide ecosystem services being important recreation tourism icons but, at the same time, are  
38 among the most damaged natural ecosystems worldwide (Hall, 2001). The over-crowding at the  
39 beaches increases the anthropogenic pressure on the adjacent marine coastal zone, leading to  
40 deterioration of water quality and aquatic life (Garcia and Servera, 2003; Hall, 2001). The  
41 potential consequent impairment of coastal ecosystem services necessarily triggers a vicious  
42 circle that, inevitably, will damage the tourism industry itself (Drius et al., 2019).

43 One of the main threats potentially driven by coastal tourism is the increase in organic and  
44 nutrient load linked to the abrupt rise in population during the high tourism season. Especially  
45 when sewage treatment systems are absent, inadequate or malfunctioning, excess input of  
46 organic matter and nutrients may enter the marine coastal areas, thereby leading to  
47 eutrophication, which may be followed by several secondary detrimental effects (Castro et al.,  
48 2007; Nixon, 1995; Signa et al., 2015).

49 Suitable approaches to track the excess of nutrients of anthropic origin in marine coastal areas  
50 include the use of macroalgae, which are proper biological indicators, due to their high uptake  
51 and assimilation rate of bioavailable nutrients (Hurd et al., 2014), together with their wide  
52 distribution, abundance and sessile life (Cole et al., 2005). In this context, an appropriate

53 technique to assess the presence and the extent of anthropic nutrients in macroalgae exposed to  
54 nutrient-enriched seawater is the analysis of nitrogen stable isotope ratio ( $\delta^{15}\text{N}$ ). Stable isotopes  
55 of nitrogen and carbon represent powerful and highly informative tools that have been widely  
56 used in environmental studies and food web ecology to trace the origin of nutrients and organic  
57 matter in natural systems (Castro et al., 2007; Signa et al., 2012; Vizzini and Mazzola, 2006). In  
58 particular,  $\delta^{15}\text{N}$  is useful in the identification of nitrogen sources entering marine ecosystems  
59 (e.g. atmospheric deposition, wastewater, fertilizers), as marine, terrestrial and anthropogenic  
60 nutrients and organic matter have different  $\delta^{15}\text{N}$  signatures (Castro et al., 2007; Cole et al., 2005;  
61 Olsen et al., 2010). Anthropogenic nitrogen is typically more  $^{15}\text{N}$ -enriched than terrestrial and  
62 marine sources due to the isotopic fractionation that occurs during nitrogen transformations (e.g.  
63 ammonia volatilisation and denitrification) and leaves the residual nitrogen pool enriched in  $^{15}\text{N}$   
64 (Heaton, 1986). In this context, marine macroalgae are able to integrate spatial and temporal  
65 variability of  $\delta^{15}\text{N}$  of dissolved nitrogen and their isotopic composition provides information on  
66 the origin of nitrogen exploited (natural vs. anthropogenic) (Cole et al., 1995, 2005; Costanzo et  
67 al., 2001).

68 If  $\delta^{15}\text{N}$  of naturally growing macroalgae is broadly used to monitor anthropogenic nitrogen input  
69 into aquatic ecosystems (e.g. Derse et al., 2007; Lin et al., 2007; Morris et al., 2009; Savage et  
70 al., 2005), a step beyond is represented by the deployment approach consisting in short-term  
71 macroalgae incubations in selected areas to assess the change of their  $\delta^{15}\text{N}$  values over the  
72 deployment period, according to local environmental conditions (e.g. Costanzo et al., 2001;  
73 García-Seoane et al., 2018). The main advantages of this approach, compared with the analysis  
74 of naturally occurring macroalgae, derive from the wide coverage of the area that can be  
75 monitored, coupled with a low spatial variability of the initial macroalgae  $\delta^{15}\text{N}$ , as the algae used

76 for the deployment are collected from the same site of origin (Alquezar et al., 2013) and the  
77 known period of exposure (García-Seoane et al., 2018). This approach was successfully set up in  
78 many areas worldwide to detect and map anthropogenic nutrient sources and plumes, especially  
79 in case of potential sewage (Costanzo et al., 2005, 2001), agricultural (Deutsch and Voss, 2006)  
80 industrial (Alquezar et al., 2013) and aquaculture (García-Sanz et al., 2011, 2010) impacts. Most  
81 of these studies used the opportunistic bloom-forming Chlorophyta *Ulva* spp. because of its  
82 acknowledged high nitrogen removal efficiency and incorporation rate (Pedersen and Borum,  
83 1997) that ensure a rapid and efficient response to nutrient enrichment. Nevertheless,  
84 experimental manipulation of opportunistic macroalgae suffers from two main constraints: i)  
85 availability and biomass may strongly vary across the year (García-Seoane et al., 2018); ii) they  
86 need a preliminary acclimation step in oligotrophic seawater to allow a complete  
87 turnover/depletion of the internal nitrogen pool (Dailer et al., 2010; Orlandi et al., 2014), as they  
88 occur prevalently in nutrient enriched areas. On the other hand, perennial macroalgae, such as  
89 Fucales, show slower nutrient uptake and growth rates than opportunistic ones (Martínez et al.,  
90 2012), but dominate in most temperate areas across the year (Mannino et al., 2014) and are more  
91 sensitive to anthropogenic disturbance (Arévalo et al., 2007; Ballesteros et al., 2007). Therefore,  
92 their use in biomonitoring studies is less frequent, although it may represent a valid potential  
93 (García-Seoane et al., 2018), especially for bypassing the acclimation step, which is not always  
94 feasible in routine monitoring.

95 Here, the genus *Cystoseira* C. Agardh was used to detect the occurrence and temporal variation  
96 of anthropogenic nutrients in coastal seawater in relation to tourist flows in three Mediterranean  
97 islands, using the deployment approach and nitrogen stable isotope analysis. We hypothesised  
98 that seasonality of tourism in Mediterranean islands may lead to a variation in anthropogenic

99 nutrients in coastal seawater that can be effectively recorded in deployed macroalgae through an  
100 increase in  $\delta^{15}\text{N}$ .

101

## 102 **2 Methods**

### 103 2.1 Study areas and experimental approach

104 The study was carried out in three Mediterranean islands: Cyprus and Sicily (Italy) in 2017 and  
105 Rhodes (Greece) in 2018 (Fig. 1).

106 The experimental campaigns, based on short-term macroalgae deployments, were conducted in  
107 three periods: putatively before the tourist period (i.e. June), during the tourist peak (i.e. August)  
108 and at the end of the tourist period (i.e. October), in three experimental sites per island. The sites  
109 were selected in order to compare a potentially impacted site (e.g. featured by popular beaches  
110 and large tourist infrastructures), hereafter Tourist site, with two reference sites where tourist  
111 activities and infrastructures are negligible (hereafter Control 1 and Control 2 sites).

112 In Cyprus (Fig. 1a), Sunrise beach, which is located in the small town of Protaras, was selected  
113 as Tourist site, while the two Control sites were identified in the southernmost rocky peninsula of  
114 Cavo Greco, which is National Forest Park since 1993 and is scantily frequented by tourists. In  
115 Sicily (Fig. 1b), Giardini Naxos beach was chosen as Tourist site, and the two Control sites  
116 where chosen along the long remote beach of Fondaco Parrino, as there are no tourist  
117 infrastructures and tourist frequency is negligible. In Rhodes (Fig. 1c), the beach of the resort  
118 village of Faliraki was selected as Tourist site and the southernmost beaches of Traganou and  
119 Afandou, which are poorly frequented by tourists, were selected as Control sites.

120 The experimental fields were constituted by georeferenced grids of 30 points (Tourist sites) and  
121 21 points (both Control sites), which were distributed, at the distance of 50 m each other, along

122 three parallel transects (T1, T2, T3). The transects were, in turn, distant 100, 200 and 300 m from  
123 the coastline in Cyprus and Rhodes and 200, 250 and 300 m in Sicily, due to differences in local  
124 regulations and restrictions posed by the competent Authorities. Each point corresponded to the  
125 exact position where the macroalgae were deployed within removable devices made of a single  
126 nylon net bag, which was anchored to the bottom with a ballast and kept straight in the water  
127 column at a depth of 1.5 m with a buoy, to ensure good light conditions. The exposure time was  
128 3 days, which is a good tradeoff that allows macroalgae to detect the spatial distribution of  $\delta^{15}\text{N}$ ,  
129 before other factors (e.g. light, siltation and biofouling) might affect their response (Costanzo et  
130 al., 2005; Huntington and Boyer, 2008).

131 Three intertidal macroalgae species of the genus *Cystoseira* were used for the experiment: based  
132 on their local availability, *C. humilis*, *C. amentacea* and *C. compressa* were chosen respectively  
133 in Cyprus, Sicily and Rhodes. The genus *Cystoseira*, one of the most representative canopy-  
134 forming Fucales (Phaeophyceae) in the Mediterranean Sea, is used as bioindicator of seawater  
135 quality due to its sensitivity to anthropogenic pressure (Ballesteros et al., 2007). Moreover  
136 *Cystoseira* species have a similar response to nutrient enrichment (Sales and Ballesteros, 2009)  
137 showing also a comparable pattern in nutrient uptake and accumulation (Sales et al., 2011).

138 In all islands, entire macroalgae thalli of the selected species were sampled before the onset of  
139 the experiment from a rocky shore characterized by overall pristine conditions, hereafter called  
140 Collection site, where the macroalga was present with high abundance throughout all the  
141 experimental periods. All collection sites, placed respectively in the Cavo Greco peninsula in  
142 Cyprus, in the locality of Addaura in Sicily and of Ladiko in Rhodes, were characterized by  
143 exposed rocky shores facing north-east, low depth (2 m maximum) and very scant presence of

144 bathers throughout the year. Moreover, the presence of allochthonous nutrient input can be ruled  
145 out at all collection sites.

146 The macroalgae collected at the Collection site were: i) analysed for  $\delta^{15}\text{N}$  to record the isotopic  
147 signature at the onset of the experiment (Day 0,  $n = 5$ ), representing the isotopic baseline to  
148 which compare the  $\delta^{15}\text{N}$  of the deployed macroalgae at the end of the experiment; ii) deployed in  
149 the Collection site using the same type of device and for the same duration as in the Tourist and  
150 Control sites with the purpose to check any effect of the experimental procedure (procedural  
151 control) on the macroalgae performance, by comparing their  $\delta^{15}\text{N}$  signature at the end of the  
152 deployment on Day 3 (Day 3 - *in situ* Control,  $n = 5$ ) with that of further samples naturally  
153 present in the Collection site and contextually collected (Day 3,  $n = 5$ ); iii) deployed in the  
154 Tourist and Control sites following the experimental design illustrated above ( $n = 72$ ).

155 At the end of the third day, the deployment devices were collected from the Tourist and Control  
156 sites, macroalgae thalli were carefully removed from the net bags, rinsed with distilled water and  
157 stored in the cold until the arrival to the laboratory. Furthermore, during both phases of  
158 deployment and retrieval of the net bags at the experimental sites, main physicochemical  
159 variables of seawater (temperature and salinity) were recorded using a multiparameter probe.  
160 Surface seawater samples were also collected in triplicate (10 L each) from each transect to  
161 obtain the total nitrogen content and the background isotopic signature of the suspended  
162 particulate organic matter (POM).

163

## 164 2.2 Sample processing and laboratory analysis

165 Once in the laboratory, only the apical portion of the frond of each thallus, corresponding to the  
166 newly grown tips, was selected for the isotopic analysis, as apical tips of perennial macroalgae



167 integrate nutrient concentration and isotopic values of seawater nutrients during their growing  
168 period (Viana and Bode, 2013). Then, apical tips were quickly rinsed with distilled water to  
169 remove any external material and gently scraped with a scalpel to remove epiphytes, when  
170 necessary. Seawater samples were prefiltered at 200 µm and then filtered on precombusted  
171 (450°C, 4h) filters (GF/F Whatman, pore size 0.45 µm) and rinsed with distilled water.  
172 Macroalgae subsamples and POM filters were then oven dried at 60°C for 48 hours and  
173 subsequently ground to a fine powder using a micro-mill. An aliquot of each ground sample was  
174 packed in tin capsules and analysed for total nitrogen (TN%) using an Elemental Analyser  
175 (Thermo Flash EA1112) and  $\delta^{15}\text{N}$  using an Isotope Ratio Mass Spectrometer (Thermo Delta  
176 IRMS Plus XP) coupled to an Elemental Analyser. Nitrogen stable isotope ratio was expressed in  
177  $\delta$  unit notation, as parts per mil deviation from the international standard (atmospheric  $\text{N}_2$ ) as  
178 follows:

$$179 \delta^{15}\text{N} = [({}^{15}\text{N}/{}^{14}\text{N}_{\text{sample}})/({}^{15}\text{N}/{}^{14}\text{N}_{\text{standard}}) - 1] \times 10^3.$$

180 Analytical precision based on the standard deviation of replicates of internal standards  
181 (International Atomic Energy Agency IAEA-CH-6) was 0.1‰.

182

### 183 2.3 Data analysis and statistics

184 Permutational univariate analysis of variance (PERMANOVA - PRIMER 6 v6.1.10 &  
185 PERMANOVA+  $\beta 20$ ; Anderson et al., 2008) was used to test for total N and  $\delta^{15}\text{N}$  differences  
186 among periods and sites in each island for the suspended particulate organic matter (POM) based  
187 on Euclidean distance matrices obtained from untransformed data. A two-factor design (factor  
188 Period fixed with three levels: June, August, October; factor Site with three levels: Tourist,  
189 Control 1, Control 2; fixed and orthogonal) was set for each island.

190  $\delta^{15}\text{N}$  values of the macroalgae collected at the Collection site in each island were compared  
191 between Periods and Days through PERMANOVA based on Euclidean distance matrices  
192 obtained from untransformed data. In particular, we tested for the isotopic variation: i) due to the  
193 experimental procedure on the macroalgae performance (by comparing Day 3-*in situ* Control vs.  
194 Day 3) and ii) naturally occurring across the same 3-days of the experiment (by comparing Day 0  
195 vs. Day 3). To do this, a two-factor design (factor Period fixed with three levels: June, August,  
196 October; factor Day with three levels: Day 0, Day 3 and Day 3 – *in situ* Control; fixed and  
197 orthogonal) was set.

198  $\delta^{15}\text{N}$  values of the deployed macroalgae were compared in each island, period, site and transect,  
199 with the correspondent baseline through t-test between independent groups (STATISTICA v.10).  
200 The baseline adopted was the mean  $\delta^{15}\text{N}$  value of the macroalgae from the Collection site at Day  
201 0 in each period, except in the case of Cyprus in October where the mean  $\delta^{15}\text{N}$  value of the  
202 macroalgae collected at Day 3 was used as baseline, due to the significant influence of the  
203 meteorological conditions (i.e. intense raining) during the 3-day deployment (see results for  
204 further details). Homogeneity of variance was previously checked through Levene test.

205 Afterwards, the isotopic variation occurred at the end of the deployment period (i.e. the  
206 difference between the  $\delta^{15}\text{N}$  of the deployed macroalgae and the  $\delta^{15}\text{N}$  of the baseline) was  
207 calculated for each sample and expressed as  $\Delta\delta^{15}\text{N}$ .

208 The relationship between the isotopic variation of the deployed macroalgae and the total nitrogen  
209 content of POM, proxy for the nitrogen load and availability in seawater (Signa et al., 2012), was  
210 explored separately by island through simple linear regression using POM TN as the independent  
211 variable and  $\Delta\delta^{15}\text{N}$  as the dependent variable. Both variables were averaged by transect.

212 Residual analysis was run to test the model assumptions and robustness and to identify potential

213 outliers. Additionally,  $\Delta\delta^{15}\text{N}$  in the Tourist site was compared with two indicators of tourist  
214 flow, hotel accommodations (only for Cyprus and Sicily) and international arrivals of passengers  
215 at the closest airport (Larnaka, Catania and Rhodes, for Cyprus, Sicily and Rhodes respectively).  
216 Tourism data have been obtained from the Ministry of Agriculture, Rural Development and  
217 Environment of Cyprus, Taormina Etna Consortium, and the Municipality of Rhodes.  
218 The analysis of spatial patterns of  $\Delta\delta^{15}\text{N}$  was conducted through Quantum GIS (version 2.18.7)  
219 using the Inverse distance weighted (IDW) interpolation technique, which allows to determine  
220 cell values using a linearly weighed combination of a set of sample points where the weight is a  
221 function of inverse distance (Philip and Watson, 1982; Watson and Philip, 1985). With the  
222 purpose to realize a tool for transferring complex ecological information to competent  
223 authorities,  $\Delta\delta^{15}\text{N}$  values were ranked into 5 classes (corresponding to different colours) across  
224 all the study areas, sites and periods. In more detail, the five classes were set according to current  
225 literature concerning isotopic variation of deployed *Cystoseira* spp. (García-Sanz et al., 2011,  
226 2010; Orlandi et al., 2014); the contours of these 5 categories indicate the occurrence and the  
227 extent of plumes of  $^{15}\text{N}$ -enriched [ $\Delta\delta^{15}\text{N}$  positive values: warm colour scale with 4 classes  
228 indicating low (0-0.5‰), moderate (0.5-1‰), high (1-1.5‰) or very high (> 1.5‰) isotopic  
229 enrichment] vs.  $^{15}\text{N}$ -depleted [ $\Delta\delta^{15}\text{N}$  negative values: cold colour with 1 class indicating  
230 variations < 0‰] nutrients in the coastal sites over the experimental periods.

231

## 232 3 Results

### 233 3.1 Environmental characterization

234 Temperature and salinity followed a common temporal trend in Cyprus, Sicily and Rhodes. In  
235 particular, both seawater temperature and salinity varied similarly across the three sites of each  
236 island, increasing from June to August, and decreasing in October (Table 1).

237 Mean total N of suspended particulate organic matter (POM) showed the highest values and  
238 higher temporal variability in Sicily peaking in August in all sites (Fig. 2, Appendix S1). POM  
239 TN content in Rhodes was higher in August and at the Tourist site than in the others periods and  
240 sites. In contrast, no temporal or spatial differences were highlighted in Cyprus (Fig. 2, Appendix  
241 S1). In both Cyprus and Sicily, mean POM  $\delta^{15}\text{N}$  peaked in August in the Tourist site and then  
242 significantly dropped in October in both Tourist and Control sites (Fig. 2, Appendix S2). Also in  
243 Rhodes, the highest values were recorded in the Tourist site, although only before and at the end  
244 of the tourist peak (June and October), but a common pattern across sites was not identifiable  
245 (Fig. 2, Appendix S2).

246

### 247 3.2 Macroalgae incubation experiment

248 The three macroalgae species *Cystoseira humilis*, *C. amentacea* and *C. compressa*, collected  
249 from the Collection site during the different collection days (Day 0 and Day 3) respectively in  
250 Cyprus, Sicily and Rhodes, showed different  $\delta^{15}\text{N}$  values across periods, ranging respectively  
251 from -0.4 to 1.2 ‰ (mean value  $0.5 \pm \text{s.d. } 0.4\text{‰}$ ), from 6.7 to 7.7 ‰ ( $7.3 \pm 0.3\text{‰}$ ) and from 1.6  
252 to 3.5 ‰ ( $2.2 \pm 0.4\text{‰}$ ).

253 Permutational univariate analysis of variance (PERMANOVA) revealed significant differences  
254 in the macroalgae  $\delta^{15}\text{N}$  values for the interaction of the factors Period and Day at the Collection

255 site in all islands (Cyprus:  $F_{(4, 36)} = 10.7$ ,  $p = 0.001$ ; Sicily:  $F_{(4, 36)} = 5.1$ ,  $p = 0.019$ ; Rhodes:  $F_{(4, 36)}$   
256  $= 4.3$ ,  $p = 0.004$ , Appendix S3). Nevertheless, in all islands and periods, the comparison between  
257  $\delta^{15}\text{N}$  values of the macroalgae collected at Day 3 and the procedural control (Day 3 – *in situ*  
258 Control) showed no significant differences ( $p > 0.05$ , Appendix S3), indicating that the  
259 experimental procedure did not influence the  $\delta^{15}\text{N}$  signature of the macroalgae. In contrast, the  
260 comparison between Day 0 and Day 3 revealed significant differences only in Cyprus in  
261 October, with significantly higher  $\delta^{15}\text{N}$  at Day 0 than at Day 3 probably due to intense raining  
262 occurred during the experiment implementation, which, passing through agricultural fields, may  
263 have contributed to runoff of  $^{15}\text{N}$ -depleted nitrogen. Consequently, to remove the effect of this  
264 natural variability, the mean  $\delta^{15}\text{N}$  value of the macroalgae collected at Day 3 (instead of those  
265 collected at Day 0) was set as baseline to which compare the  $\delta^{15}\text{N}$  of the deployed macroalgae at  
266 the end of the experiment. Similarly, the higher  $\delta^{15}\text{N}$  observed at Day 0 in October in Sicily and  
267 Rhodes, compared with the other periods, may be due to adverse weather and sea conditions  
268 during the days immediately before the experiment, as rainfall and high water mixing may have  
269 led to  $^{15}\text{N}$ -enriched nitrate replenishment in the upper water layer (Michener and Shell, 1994).  
270 Nitrogen stable isotope signature  $\delta^{15}\text{N}$ , total nitrogen TN and C/N ratio of the macroalgae  
271 selected as baseline are showed in Table 2. Although the inter-island variability in  $\delta^{15}\text{N}$ , with the  
272 lowest values in Cyprus, followed by Rhodes and then Sicily with the highest values, TN was  
273 overall in a narrow range, varying from  $0.7 \pm 0.1\%$  in Cyprus to  $1.3 \pm 0.2\%$  in Sicily.  
274 Accordingly, the higher C/N ratio ( $> 40$ ) were recorded in Cyprus, while in Sicily and Rhodes it  
275 ranged overall from 20 to 40 (Table 2) .  
276 The comparison between the  $\delta^{15}\text{N}$  values of the macroalgae deployed at increasing distance from  
277 the coastline in each island, site and period, and the baseline  $\delta^{15}\text{N}$ , revealed a significant isotopic

278 enrichment at the end of the 3-day deployment in the Tourist site of Cyprus in all the periods  
279 (Fig. 3a). In contrast, macroalgae deployed in Sicily and Rhodes, showed a significant isotopic  
280 enrichment at the end of the deployment only in the Tourist site during the tourist peak (August)  
281 in transects 1 and 2 in Sicily and only transect 1 in Rhodes. A significant  $^{15}\text{N}$  depletion was  
282 recorded in the macroalgae deployed in June at the Control 1 in Sicily (transect 1 and 3) and  
283 Rhodes (transect 3) and in October at all sites of Rhodes (transect 1 at the Tourist site, transect 2  
284 at the Control 1 and transect 3 at the Control 2) (Fig. 3b, c).

285 Looking at the variation of  $\delta^{15}\text{N}$  in the macroalgae tissues at the end of the deployment, hereafter  
286  $\Delta\delta^{15}\text{N}$ , georeferenced maps show the temporal and spatial  $\Delta\delta^{15}\text{N}$  trends recorded in the three  
287 islands (Figs. 4, 5 and 6), with a slight wider  $\Delta\delta^{15}\text{N}$  range in Sicily (2.37‰: from -1.16 to  
288 1.21‰) than in Rhodes (2.05‰: from -1.36 to 0.69‰) and Cyprus (1.79‰: from -0.43 to  
289 1.36‰). In Cyprus, an isotopic enrichment was evident in the landward transect (100 m from the  
290 coastline) of the Tourist site in June and October, and then spread up to transect 3 (300 m from  
291 the coastline) in August, when also some  $\Delta\delta^{15}\text{N}$  peaks were recorded in the landward transect. In  
292 contrast, at both Control sites, there was only a very small isotopic variation in macroalgae, with  
293 low positive or negative  $\Delta\delta^{15}\text{N}$  values (Fig. 4). At the Tourist site in Sicily, positive  $\Delta\delta^{15}\text{N}$   
294 values were evident in the macroalgae deployed in August, especially in the southern part of the  
295 bay, where a few enrichment peaks were recorded. In contrast, an overall decrease in the isotopic  
296 values of the deployed macroalgae was detected in June, and in both Control sites in August. In  
297 October, a minor isotopic variations occurred in the deployed macroalgae, except for the  
298 southern part of Giardini Naxos bay, where a slight isotopic enrichment persisted (Fig. 5). Lastly,  
299 the maps of Rhodes clearly show that only a low enrichment characterized the high season  
300 (August) at the Tourist site, and somewhat spread within 100 m at the Control 1 site, while

301 during the other two periods an overall isotopic depletion in the macroalgae tissues occurred at  
302 all sites (Fig. 6).

303 Linear regression analysis revealed that  $\Delta\delta^{15}\text{N}$  of the deployed macroalgae significantly  
304 increased with increasing POM TN content in Cyprus and Sicily (Cyprus:  $y = 0.045 + 0.016x$ ,  
305  $R^2 = 0.43$ , p-value = 0.008; Sicily:  $y = 0.139 + 0.143x$ ,  $R^2 = 0.35$ , p-value = 0.001). In contrast,  
306 no significant linear relation emerged in Rhodes ( $y = 0.053 + 0.015x$ ,  $R^2 = 0.09$ , p-value = 0.07).  
307 Moreover, mean  $\Delta\delta^{15}\text{N}$  of the macroalgae deployed in the Tourist sites showed a different trend  
308 in the three islands, being overall comparable across periods in Cyprus, peaking in August in  
309 Sicily, and dropping in October in Rhodes (Fig. 7). Although data about hotel accommodations  
310 are missing in Rhodes, these  $\Delta\delta^{15}\text{N}$  trends are overall consistent with the tourist flow data, which  
311 revealed a high number of visitors in Cyprus and Rhodes since June with a decrease, more  
312 marked in Rhodes, in October and a peak in August in Sicily (Fig. 7).

313

#### 314 **4 Discussion**

315  $\delta^{15}\text{N}$  of macroalgae is known to be a useful proxy for anthropogenic nutrients presence in coastal  
316 seawater (e.g. Cole et al. 2005, Costanzo et al. 2005, Hurd et al. 2014, García-Seoane et al. 2018)  
317 and well before that main ecological changes become observable. Although opportunistic green  
318 macroalgae are acknowledged as good indicators of nitrogen supply and sources in coastal  
319 systems (Fernandes et al., 2012; Orlandi et al., 2014), this study confirms that also brown  
320 macroalgae are reliable indicators of anthropogenic nutrient input in coastal areas through  
321 deployment techniques (Alquezar et al., 2013).

322 The isotopic variation,  $\Delta\delta^{15}\text{N}$ , occurred in *Cystoseira* species at the end of the 3-day deployment  
323 period showed relevant spatial and temporal patterns, as well as island-specific differences,

324 which provided indication of the presence of anthropogenic nitrogen nutrients in seawater. This  
325 is because macroalgae typically uptake heavier isotopes ( $^{15}\text{N}$ ) when they are more available,  
326 quickly integrating them into their tissues (Cole et al., 2005; Costanzo et al., 2001; Fernandes et  
327 al., 2012) and show very little or no fractionation during N-uptake and assimilation, unless  
328 exposed to high nitrate concentrations (Gröcke et al., 2017; Swart et al., 2014). Although we did  
329 not analyse the concentration of nitrogen compounds in seawater, the very low nitrogen content  
330 ( $< 0.4\%$ ) of the particulate organic matter (POM) in all the islands indicates that the coastal  
331 areas studied are oligotrophic across all periods.

332 In Cyprus, the  $\Delta\delta^{15}\text{N}$  pattern was very evident, and revealed a higher isotopic enrichment in the  
333 macroalgae deployed in August than in June and October. Moreover, this pattern was especially  
334 evident in the Tourist site, where  $\Delta\delta^{15}\text{N}$  also decreased at increasing distance from the coast.

335 These findings give a clear clue of the origin and the timing of anthropogenic nutrient spread,  
336 which, as expected, seems strictly associated to coastal inputs, thereby to tourism activities.

337 Indeed, tourist arrival in Cyprus starts early in spring and gradually increases up to the peak in  
338 August, and then starts to drop from September. Moreover, in the Tourist site investigated in  
339 Cyprus, many leisure activities are offered to the beach users, such as lidos, watercrafts and  
340 water sports, and the whole town is surrounded by tourist facilities such as restaurants, hotels and  
341 resorts, whose guests, along with international arrivals by flight, follow the same temporal  
342 pattern as  $\Delta\delta^{15}\text{N}$ . Seasonality of tourism seems to exert a detectable effect on  $\delta^{15}\text{N}$  of  
343 macroalgae, with an evident enrichment, although overall moderate ( $< 1.4\%$ ), compared to the  
344 baseline recorded at the beginning of the tourist flow, in June, peaking in August, during the  
345 tourist peak, and then decreasing at the end of the tourist season. In contrast, the Cavo Greco  
346 peninsula, where Control sites were placed, hosts a protected National Forest Park and



347 agricultural fields, hence no infrastructures are present; tourist attendance is very low even  
348 during the high season, and limited to local people and small tourist cruise ships that stop in the  
349 coastal area during daily excursions. Accordingly, a low isotopic enrichment was detected in the  
350 macroalgae deployed at both Control sites across the periods.

351 These findings are in accordance with both nitrogen content and isotopic signature of the  
352 suspended particulate organic matter (POM) recorded in the coastal waters of Cyprus. The  
353 temporal pattern of POM  $\delta^{15}\text{N}$  (i.e. higher at the Tourist site in August than in October and in the  
354 Control sites in both periods), as well as the positive correlation between the  $\Delta\delta^{15}\text{N}$  of the  
355 deployed macroalgae and the POM TN content, suggests the relationship between the presence  
356 of anthropogenic nutrients and the macroalgae response at the Tourist site.

357 The suspended POM in coastal seawater is generally composed by a mixture of detrital material  
358 and living phytoplankton, which are known to quickly uptake dissolved nutrients, and then  
359 responds to the nutrient load and typology with variations in N content and  $\delta^{15}\text{N}$  respectively  
360 (Signa et al., 2012; Vizzini and Mazzola, 2006). In particular, POM isotopic signature is widely  
361 recognized to give indication of the trophic condition of the environment, including the presence  
362 of anthropogenic input or events of eutrophication (Cole et al., 2005; Signa et al., 2012).

363 Although the increase in  $\delta^{15}\text{N}$  signature of dissolved and particulate nutrients is linked to a  
364 number of chemical and biological processes, among which nitrification from excess  
365 sewage/nutrient runoff, denitrification or organic decomposition by bacteria and ammonia  
366 enrichment from industrial discharges (Costanzo et al., 2005, 2001), we can suppose that direct  
367 nutrient enrichment from bathing activities, and potentially undersized wastewater management  
368 from the horeca (hotels, restaurants, cafes) infrastructures during the tourist peak may have led to  
369 the observed patterns.

370 Similarly to Cyprus, the isotopic patterns of the macroalgae deployed in Sicily suggest that the  
371 coastal activities of the tourist beach of Giardini Naxos represent a source of anthropogenic  
372 nutrients into the bay, although mostly restricted to August. The summer increase in tourists and  
373 bathers at the beach, coupled with several recreational water activities (boating, water sports) and  
374 tourist facilities (hotels, restaurants and private houses) may be responsible for this small-spatial  
375 scale pattern, despite the extent of variation is quite moderate. In particular, the presence of a  
376 tourist port and breakwaters at the southeastern side may have led to a localised higher  
377 availability of  $^{15}\text{N}$ -enriched nutrients, which is slightly evident also in October, most probably  
378 due to a reduction of the water exchange in the area. Moreover, the macroalgae seasonal trend  
379 was exactly consistent with that of POM nitrogen content and isotopic signature, which indeed  
380 showed a peak in August, confirming a localised derived increase in  $^{15}\text{N}$ -enriched nutrients in the  
381 area.

382 Unlike the aforementioned islands, and although the high tourist flow interesting the island of  
383 Rhodes both in June and August, and big resorts located in the beach front of the Tourist site,  
384 both the temporal and spatial variability of the isotopic values of the deployed macroalgae were  
385 fairly low.  $\delta^{15}\text{N}$  of the macroalgae showed only a low isotopic enrichment in August at all  
386 transects of the Tourist site and in the landward transect of one control site. In all the other sites  
387 and periods, no enrichment was recorded by macroalgae, indicating that anthropic nutrients were  
388 not recordable. Also the POM isotopic value did not show a clear pattern: although  $\delta^{15}\text{N}$  was  
389 higher in the Tourist site than in Controls, it was lower in August than in June and October,  
390 contrarily to expectations. Moreover, although the nitrogen content of POM was significantly  
391 higher in August than in June, the lack of correlation with the isotopic variation of deployed  
392 macroalgae rules out the anthropic origin of nutrient load recorded. Therefore, despite the

393 presence of numerous tourist facilities along the coast, the demographic increase and the many  
394 leisure activities including bathing, boating and water sports, a negligible input of  $^{15}\text{N}$ -enriched  
395 nutrients occurred in shallow coastal waters in June and August, and no evident spread of  
396 anthropogenic nutrients up to offshore areas was highlighted, suggesting that management of  
397 tourism and wastewater seems to be efficient also during the tourist peak.

398 Turning to the extent of the isotopic variation detected in the macroalgae across periods, sites  
399 and transects, overall modest variations were recorded,  $\delta^{15}\text{N}$  enrichments ( $\Delta\delta^{15}\text{N}$ ) did not exceed  
400 1.4‰ in Cyprus, 1.2‰ in Sicily and 0.7‰ in Rhodes, and were comparable with previous  
401 deployment studies that used species of the *Cystoseira* genus. Among these, Orlandi et al. (2014)  
402 found an isotopic enrichment up to +1.7‰ of *C. amentacea* incubated for 48 hours in a strongly  
403 urbanised coastal area impacted by polluted river discharge. The highest  $\Delta\delta^{15}\text{N}$  found in Cyprus  
404 and Sicily was within the range reported by Orlandi et al. (2014), further confirming the uptake  
405 of  $^{15}\text{N}$ -enriched nutrients by the deployed macroalgae. However, only a few macroalgae samples  
406 showed values similar to the highest peaks recorded by Orlandi et al. (2014), not indicating a  
407 marked presence of anthropogenic nutrients.

408 At the same time, the minor isotopic enrichment found in Rhodes is most likely the result of a  
409 negligible influence of input of anthropic origin. In contrast, García-Sanz et al. (2010, 2011)  
410 found only a low to moderate isotopic enrichment (up to +0.8‰ and +0.7‰ respectively) in *C.*  
411 *mediterranea* deployed at a depth of 5 m for 4–6 days at increasing distance from a fish farm.

412 Although aquaculture waste is a common cause of  $^{15}\text{N}$  enrichment in aquatic environments  
413 (Vizzini and Mazzola, 2004), the authors attributed the small enrichment to the high baseline  
414 values of the macroalgae, coupled with a high nitrogen content, that may have masked the effects  
415 of spatial nutrient gradients from fish farms. Although we also recorded a high isotopic baseline

416 in Sicily, we rule out that this may have biased the macroalgae nutrient uptake, as it was not  
417 coupled with a high nitrogen content. Rather, in spite of the inter-island baseline variability that  
418 may be ascribed to intrinsic background oceanographic factors independent on human activity  
419 (Viana and Bode, 2013; Vizzini et al., 2011), low TN content and high C/N ratio were observed  
420 in all the macroalgae used as baseline, consistent with previous studies on *Cystoseira* species  
421 from oligotrophic coastal areas (Celis-Plá et al., 2014). TN and C/N ratio respectively below and  
422 above the critical values of 2% and 10, like those observed in this study, indicate N-limitation  
423 (Phillips and Hurd, 2003), condition where high uptake rates are usually observed. In particular,  
424 intertidal macroalgae are able to maximize nitrogen acquisition independent on the available  
425 nitrogen form, as a strategy to cope with the highly variable and potentially N-limited coastal  
426 environment (Phillips and Hurd, 2004).

427 Although the comparison of the three *Cystoseira* species was out of the scope of the present  
428 study, assuming a similar response to nutrient enrichment by the three species used (*C. humilis* in  
429 Cyprus, *C. amentacea* in Sicily and *C. compressa* in Rhodes), the match among the temporal  
430 pattern of  $\Delta\delta^{15}\text{N}$  in macroalgae,  $\delta^{15}\text{N}$  in POM and visitor flows, and the correlation between  
431  $\Delta\delta^{15}\text{N}$  in macroalgae and the nitrogen content of POM i) suggests the reliability of *Cystoseira*  
432 genus in deployment experiments; ii) confirms the greater usefulness of the deployment  
433 approach compared to standard monitoring based on nutrients and/or POM characterization.  
434 Indeed, although more time consuming, the biomonitoring approach using  $\delta^{15}\text{N}$  of deployed  
435 macroalgae provides space- and time-integrated information about anthropogenic impact, while  
436 the analysis of nutrients and/or POM might only provide a snapshot of the highly variable water  
437 column conditions.

438 As previously mentioned, macroalgae widely differ according to their nutritional needs and  
439 growth strategy, as well as nutrient metabolism (Pedersen and Borum, 1997). In this context,  
440 perennial and slow-growing macroalgae, such as Cystoseiraceae (Phaeophyta) (Mannino et al.,  
441 2017), are overall characterized by lower turnover and uptake rates, and have developed nutrient  
442 storage pools to cope with low nutrient availability (Martínez et al., 2012). Differently,  
443 opportunistic and fast-growing Ulvaceae (Chlorophyta) have a high ability to accumulate and  
444 store available nutrients in excess and are characterized by high nutrient uptake and growth rates  
445 (Fong et al., 2004; Lubsch and Timmermans, 2018). This opposite metabolism is certainly  
446 responsible of the very high isotopic enrichment found in the green macroalga *Ulva* spp. used in  
447 other deployment experiments (e.g. from +28 to +45‰ in Dailer et al. 2010 and from +10 to  
448 +14‰ in Dailer et al. 2012), as well as the different response of *Cystoseira* vs. *Ulva* ( $\Delta\delta^{15}\text{N}$   
449 range: +0.5 - +1.7 ‰ and +1.5 - +4.3 ‰ for *Cystoseira* and *Ulva* respectively) incubated in the  
450 same anthropized site highlighted by Orlandi et al. (2014).

451 Nevertheless, field and laboratory experiments reported rapid and significant response of  
452 different *Cystoseira* species, once exposed to higher nutrient concentrations. In more detail,  
453 Celis-Plá et al. (2014) observed increase in nitrogen content, phenolic compounds and  
454 carotenoids in *C. tamariscifolia*. Similarly, Vaz-Pinto et al. (2014), exposing *C. humilis* to high  
455 nutrient concentrations in laboratory conditions, found higher growth and nutrient uptake rates  
456 than those reported for other perennial species. Lastly, *C. compressa* was found to respond well  
457 to high nutrient conditions (Celis-Plá et al., 2015) and to bioaccumulate trace elements (Benfares  
458 et al., 2015), confirming its suitability as a biomarker of pollution in coastal areas.

459

460 **Conclusion**

461 Main findings of this study showed that the manipulative deployment approach with brown  
462 macroalgae of the genus *Cystoseira* worked effectively in the detection and monitoring of  
463 anthropogenic nutrient enrichment in marine coastal areas driven by tourism activities. However,  
464 despite the spatial and temporal patterns emerged in macroalgae  $\Delta\delta^{15}\text{N}$ , its overall extent was  
465 rather low or moderate, with only a few high enrichment peaks, depending on the specific site  
466 investigated. This suggests a modest influence of anthropogenic activities on nutrient input in  
467 coastal seawater in Cyprus and Sicily, which was instead negligible in Rhodes. The final output  
468 consisting in georeferenced maps, indeed, summarizes important information that is relatively  
469 easy to read and to transfer to competent authorities, helping in facing the major issue of  
470 deterioration of water quality due to tourism impact and the consequent impairment of ecosystem  
471 services in highly tourist areas. As many aspects of the coastal economy are dependent upon the  
472 environmental preservation and recreational quality of the beaches, this approach can represent  
473 an early warning system for the development of adequate management plans for a sustainable  
474 coastal tourism.

475

476 **Acknowledgements**

477 The research was funded by the INTERREG MED- BLUEISLANDS (Seasonal variation of  
478 waste as effect of tourism. Ref: 613 / 1MED15\_3.1\_M12\_273). We are grateful to all the people  
479 who have helped to carry out the experiments of this study, in particular the project partners for  
480 their support in each island and all the trainers involved. In particular, we thank the Department  
481 of Environment of the Ministry of Agriculture, Rural Development and Environment of Cyprus  
482 (especially the Environmental Officer Athena Papanastasiou), InteliConS (the Managing

483 Director Loizos Afxentiou and the collaborators Andreas Symeonides and Lambros  
484 Palambrianou), the Taormina Etna Consortium (especially Salvatore Spartà and Oreste Lo  
485 Basso), the Municipality of Rhodes (especially the Mayor Advisor on Water Resources and  
486 Environmental Management Christos C. Gamvroudis). We are also grateful to all the LaBioMar  
487 (University of Palermo) staff, and, in particular, to Fabio D’Addelfio, Andrea Savona, Veronica  
488 Santinelli, Valentina Scutteri and Cecilia Tramati for their lab and field support, and Elisa A.  
489 Aleo for help with laboratory analyses.

490

#### 491 **References**

- 492 Alquezar, R., Glendenning, L., Costanzo, S., 2013. The use of the brown macroalgae, *Sargassum*  
493 *flavicans*, as a potential bioindicator of industrial nutrient enrichment. Mar. Pollut. Bull. 77,  
494 140–146. doi:10.1016/j.marpolbul.2013.10.013
- 495 Anderson, M.J., Gorley, R.N., Clarke, K.R., 2008. PERMANOVA+ for PRIMER: Guide to  
496 Software and Statistical Methods, in: PRIMER-E. Plymouth, UK, pp. 1–214.  
497 doi:10.13564/j.cnki.issn.1672-9382.2013.01.010
- 498 Arévalo, R., Pinedo, S., Ballesteros, E., 2007. Changes in the composition and structure of  
499 Mediterranean rocky-shore communities following a gradient of nutrient enrichment:  
500 Descriptive study and test of proposed methods to assess water quality regarding  
501 macroalgae. Mar. Pollut. Bull. 55, 104–113. doi:10.1016/j.marpolbul.2006.08.023
- 502 Ballesteros, E., Torras, X., Pinedo, S., García, M., Mangialajo, L., de Torres, M., 2007. A new  
503 methodology based on littoral community cartography dominated by macroalgae for the  
504 implementation of the European Water Framework Directive. Mar. Pollut. Bull. 55, 172–  
505 180. doi:10.1016/j.marpolbul.2006.08.038

506 Benfares, R., Seridi, H., Belkacem, Y., Inal, A., 2015. Heavy Metal Bioaccumulation in Brown  
507 Algae *Cystoseira compressa* in Algerian Coasts, Mediterranean Sea. *Environ. Process.* 2,  
508 429–439. doi:10.1007/s40710-015-0075-5

509 Castro, P., Valiela, I., Freitas, H., 2007. Eutrophication in Portuguese estuaries evidenced by  
510  $\delta^{15}\text{N}$  of macrophytes. *Mar. Ecol. Prog. Ser.* 351, 43–51. doi:10.3354/meps07173

511 Celis-Plá, P.S.M., Hall-Spencer, J.M., Horta, P.A., Milazzo, M., Korbee, N., Cornwall, C.E.,  
512 Figueroa, F.L., 2015. Macroalgal responses to ocean acidification depend on nutrient and  
513 light levels. *Front. Mar. Sci.* 2. doi:10.3389/fmars.2015.00026

514 Celis-Plá, P.S.M., Martinez, B., Quintano, E., García-Sánchez, M., Pedersen, A., Navarro, N.P.,  
515 Copertino, M.S., Mangaiyarkarasi, N., Mariath, R., Figueroa, F.L., Korbee, N., 2014. Short-  
516 term ecophysiological and biochemical responses of *Cystoseira tamariscifolia* and  
517 *Ellisolandia elongata* to environmental changes. *Aquat. Biol.* 22, 227–243.  
518 doi:10.3354/ab00573

519 Cole, M.L., Kroeger, K.D., McClelland, J.W., Valiela, I., 2005. Macrophytes as indicators of  
520 land-derived wastewater: Application of a  $\delta^{15}\text{N}$  method in aquatic systems. *Water Resour.*  
521 *Res.* 41, 1–9. doi:10.1029/2004WR003269

522 Cole, M.L., Valiela, I., Kroeger, K.D., Tomasky, G.L., Cebrian, J., Wigand, C., Mckinney, R.A.,  
523 Grady, S.P., Carvalho de Silva, M.H., Carvalho da Silva, M.H., 1995. Assessment of a  $\delta^{15}\text{N}$   
524 isotopic method to indicate anthropogenic eutrophication in aquatic ecosystems. *J. Environ.*  
525 *Qual.* 33, 124–132. doi:10.2134/jeq2004.1240

526 Costanzo, S.D., O'Donohue, M.J., Dennison, W.C., Loneragan, N.R., Thomas, M., 2001. A new  
527 approach for detecting and mapping sewage impacts. *Mar. Pollut. Bull.* 42, 149–156.  
528 doi:10.1016/S0025-326X(00)00125-9



529 Costanzo, S.D., Udy, J., Longstaff, B., Jones, A., 2005. Using nitrogen stable isotope ratios  
530 ( $\delta^{15}\text{N}$ ) of macroalgae to determine the effectiveness of sewage upgrades: Changes in the  
531 extent of sewage plumes over four years in Moreton Bay, Australia. *Mar. Pollut. Bull.* 51,  
532 212–217. doi:10.1016/j.marpolbul.2004.10.018

533 Dailer, M.L., Knox, R.S., Smith, J.E., Napier, M., Smith, C.M., 2010. Using  $\delta^{15}\text{N}$  values in algal  
534 tissue to map locations and potential sources of anthropogenic nutrient inputs on the island  
535 of Maui, Hawai'i, USA. *Mar. Pollut. Bull.* 60, 655–671.  
536 doi:10.1016/j.marpolbul.2009.12.021

537 Dailer, M.L., Ramey, H.L., Saephan, S., Smith, C.M., 2012. Algal  $\delta^{15}\text{N}$  values detect a  
538 wastewater effluent plume in nearshore and offshore surface waters and three-dimensionally  
539 model the plume across a coral reef on Maui, Hawai'i, USA. *Mar. Pollut. Bull.* 64, 207–  
540 213. doi:10.1016/j.marpolbul.2011.12.004

541 Davenport, J., Davenport, J.L., 2006. The impact of tourism and personal leisure transport on  
542 coastal environments: A review. *Estuar. Coast. Shelf Sci.* 67, 280–292.  
543 doi:10.1016/j.ecss.2005.11.026

544 Derse, E., Knee, K.L., Wankel, S.D., Kendall, C., Berg, C.J., Paytan, A., 2007. Identifying  
545 sources of nitrogen to Hanalei Bay, Kauai, utilizing the nitrogen isotope signature of  
546 macroalgae. *Environ. Sci. Technol.* 41, 5217–5223. doi:10.1021/es0700449

547 Deutsch, B., Voss, M., 2006. Anthropogenic nitrogen input traced by means of  $\delta^{15}\text{N}$  values in  
548 macroalgae: Results from in-situ incubation experiments. *Sci. Total Environ.* 366, 799–808.  
549 doi:10.1016/j.scitotenv.2005.10.013

550 Drius, M., Bongiorno, L., Depellegrin, D., Menegon, S., Puggnetti, A., Stifter, S., 2019. Tackling  
551 challenges for Mediterranean sustainable coastal tourism: An ecosystem service

552 perspective. *Sci. Total Environ.* 652, 1302–1317. doi:10.1016/j.scitotenv.2018.10.121

553 Fernandes, M., Bengler, S., Sharma, S.K., Gaylard, S., Kildea, T., Hoare, S., Braley, M., Irving,  
554 A.D., 2012. The use of  $\delta^{15}\text{N}$  signatures of translocated macroalgae to map coastal nutrient  
555 plumes: improving species selection and spatial analysis of metropolitan datasets. *J.*  
556 *Environ. Monit.* 14, 2399–2410. doi:10.1039/c2em10997b

557 Fong, P., Fong, J.J., Fong, C.R., 2004. Growth, nutrient storage, and release of dissolved organic  
558 nitrogen by *Enteromorpha intestinalis* in response to pulses of nitrogen and phosphorus.  
559 *Aquat. Bot.* 78, 83–95. doi:10.1016/j.aquabot.2003.09.006

560 García-Sanz, T., Ruiz-Fernández, J.M., Ruiz, M., García, R., González, M.N., Pérez, M., 2010.  
561 An evaluation of a macroalgal bioassay tool for assessing the spatial extent of nutrient  
562 release from offshore fish farms. *Mar. Environ. Res.* 70, 189–200.  
563 doi:10.1016/j.marenvres.2010.05.001

564 García-Sanz, T., Ruiz, J.M., Pérez, M., Ruiz, M., 2011. Assessment of dissolved nutrients  
565 dispersal derived from offshore fish-farm using nitrogen stable isotope ratios ( $\delta^{15}\text{N}$ ) in  
566 macroalgal bioassays. *Estuar. Coast. Shelf Sci.* 91, 361–370.  
567 doi:10.1016/j.ecss.2010.10.025

568 García-Seoane, R., Aboal, J.R., Boquete, M.T., Fernández, J.A., 2018. Biomonitoring coastal  
569 environments with transplanted macroalgae : A methodological review. *Mar. Pollut. Bull.*  
570 135, 988–999. doi:10.1016/j.marpolbul.2018.08.027

571 García, C., Servera, J., 2003. Impacts of tourism development on water demand and beach  
572 degradation on the island of Mallorca (Spain). *Geogr. Ann. Ser. A Phys. Geogr.* 85A, 287–  
573 300. doi:10.1111/j.0435-3676.2003.00206.x

574 Gröcke, D.R., Racionero-Gómez, B., Marschalek, J.W., Greenwell, H.C., 2017. Translocation of

575 isotopically distinct macroalgae: A route to low-cost biomonitoring? *Chemosphere* 184,  
576 1175–1185. doi:10.1016/j.chemosphere.2017.06.082

577 Hall, C.M., 2001. Trends in ocean and coastal tourism: The end of the last frontier? *Ocean Coast.*  
578 *Manag.* 44, 601–618. doi:10.1016/S0964-5691(01)00071-0

579 Heaton, T.H.E., 1986. Isotopic studies of nitrogen pollution in the hydrosphere and atmosphere:  
580 A review. *Chem. Geol. Isot. Geosci. Sect.* 59, 87–102. doi:10.1016/0168-9622(86)90059-X

581 Huntington, B.E., Boyer, K.E., 2008. Evaluating patterns of nitrogen supply using macroalgal  
582 tissue content and stable isotopic signatures in Tomales Bay, CA. *Environ. Bioindic.* 3,  
583 180–192. doi:10.1080/15555270802537510

584 Hurd, C.L., Harrison, P.J., Bischof, K., Lobban, C.S., 2014. *Seaweed ecology and physiology.*  
585 Cambridge University Press, Cambridge (UK).

586 Lin, H.J., Wu, C.Y., Kao, S.J., Kao, W.Y., Meng, P.J., 2007. Mapping anthropogenic nitrogen  
587 through point sources in coral reefs using  $\delta^{15}\text{N}$  in macroalgae. *Mar. Ecol. Prog. Ser.* 335,  
588 95–109. doi:10.3354/meps335095

589 Lubsch, A., Timmermans, K., 2018. Uptake kinetics and storage capacity of dissolved inorganic  
590 phosphorus and corresponding N:P dynamics in *Ulva lactuca* (Chlorophyta). *J. Phycol.* 223,  
591 215–223. doi:10.1111/jpy.12612

592 Mannino, A.M., Vaglica, V., Oddo, E., 2017. Interspecific variation in total phenolic content in  
593 temperate brown algae. *J. Biol. Res.* 90, 26–29. doi:10.4081/jbr.2017.6578

594 Mannino, A.M., Vaglica, V., Oddo, E., 2014. Seasonal variation in total phenolic content of  
595 *Dictyopteris polypodioides* (Dictyotaceae) and *Cystoseira amentacea* (Sargassaceae) from  
596 the Sicilian coast. *Flora Mediterr.* 24, 39–50. doi:10.7320/FIMedit24.039

597 Martínez, B., Sordo Pato, L., Rico, J.M., Pato, L.S., Rico, J.M., Sordo Pato, L., Rico, J.M., 2012.

598 Nutrient uptake and growth responses of three intertidal macroalgae with perennial,  
599 opportunistic and summer-annual strategies. *Aquat. Bot.* 96, 14–22.  
600 doi:10.1016/j.aquabot.2011.09.004

601 Michener, R.H., Shell, D.M., 1994. Stable isotope ratios as tracers in marine aquatic food webs,  
602 in: Lajtha, K., Michener, R.H. (Eds.), *Stable Isotopes in Ecology and Environmental*  
603 *Science*. Blackwell Scientific Publications, Oxford (UK), pp. 138–157.

604 Morris, E.P., Peralta, G., Benavente, J., Freitas, R., Rodrigues, A.M., Quintino, V., Alvarez, O.,  
605 Valcárcel-Pérez, N., Vergara, J.J., Hernandez, I., Pérez-Lloréns, J.L., 2009. *Caulerpa*  
606 *prolifera* stable isotope ratios reveal anthropogenic nutrients within a tidal lagoon. *Mar.*  
607 *Ecol. Prog. Ser.* 390, 117–128. doi:10.3354/meps08184

608 Nixon, S.W., 1995. Coastal marine eutrophication: A definition, social causes, and future  
609 concerns. *Ophelia* 41, 199–219. doi:10.1080/00785236.1995.10422044

610 Olsen, Y.S., Fox, S.E., Kinney, E.L., Teichberg, M., Valiela, I., 2010. Differences in  
611 urbanization and degree of marine influence are reflected in  $\delta^{13}\text{C}$  and  $\delta^{15}\text{N}$  of producers and  
612 consumers in seagrass habitats of Puerto Rico. *Mar. Environ. Res.* 69, 198–206.  
613 doi:10.1016/j.marenvres.2009.10.005

614 Orlandi, L., Bentivoglio, F., Carlino, P., Calizza, E., Rossi, D., Costantini, M.L., Rossi, L., 2014.  
615  $\delta^{15}\text{N}$  variation in *Ulva lactuca* as a proxy for anthropogenic nitrogen inputs in coastal areas  
616 of Gulf of Gaeta (Mediterranean Sea). *Mar. Pollut. Bull.* 84, 76–82.  
617 doi:10.1016/j.marpolbul.2014.05.036

618 Pedersen, M.F., Borum, J., 1997. Nutrient control of estuarine macroalgae: Growth strategy and  
619 the balance between nitrogen requirements and uptake. *Mar. Ecol. Prog. Ser.*  
620 doi:10.3354/meps161155

621 Philip, G.M., Watson, D.F., 1982. A precise method for determining contoured surfaces. APPEA  
622 J. 22, 205–212.

623 Phillips, J.C., Hurd, C.L., 2004. Kinetics of nitrate, ammonium, and urea uptake by four  
624 intertidal seaweeds from New Zealand. J. Phycol. 40, 534–545. doi:10.1111/j.1529-  
625 8817.2004.03157.x

626 Phillips, J.C., Hurd, C.L., 2003. Nitrogen ecophysiology of intertidal seaweeds from New  
627 Zealand: N uptake, storage and utilisation in relation to shore position and season. Mar.  
628 Ecol. Prog. Ser. 264, 31–48. doi:10.3354/meps264031

629 Sales, M., Ballesteros, E., 2009. Shallow *Cystoseira* (Fucales: Ochrophyta) assemblages thriving  
630 in sheltered areas from Menorca (NW Mediterranean): Relationships with environmental  
631 factors and anthropogenic pressures. Estuar. Coast. Shelf Sci. 84, 476–482.  
632 doi:10.1016/j.ecss.2009.07.013

633 Sales, M., Cebrian, E., Tomas, F., Ballesteros, E., 2011. Pollution impacts and recovery potential  
634 in three species of the genus *Cystoseira* (Fucales, Heterokontophyta). Estuar. Coast. Shelf  
635 Sci. 92, 347–357. doi:10.1016/j.ecss.2011.01.008

636 Savage, C., 2005. Tracing the influence of sewage nitrogen in a coastal ecosystem using stable  
637 nitrogen isotopes. Ambio 34, 145–50. doi:10.1579/0044-7447-34.2.145

638 Signa, G., Mazzola, A., Costa, V., Vizzini, S., 2015. Bottom-Up Control of Macrobenthic  
639 Communities in a Guanotrophic Coastal System. PLoS One 10, e0117544.  
640 doi:10.1371/journal.pone.0117544

641 Signa, G., Mazzola, A., Vizzini, S., 2012. Effects of a small seagull colony on trophic status and  
642 primary production in a Mediterranean coastal system (Marinello ponds, Italy). Estuar.  
643 Coast. Shelf Sci. 111, 27–34. doi:10.1016/j.ecss.2012.06.008

644 Swart, P.K., Evans, S., Capo, T., Altabet, M.A., 2014. The fractionation of nitrogen and oxygen  
645 isotopes in macroalgae during the assimilation of nitrate. *Biogeosciences* 11, 6147–6157.  
646 doi:10.5194/bg-11-6147-2014

647 Vaz-Pinto, F., Martínez, B., Olabarria, C., Arenas, F., 2014. Neighbourhood competition in  
648 coexisting species: The native *Cystoseira humilis* vs the invasive *Sargassum muticum*. *J.*  
649 *Exp. Mar. Bio. Ecol.* 454, 32–41. doi:10.1016/j.jembe.2014.02.001

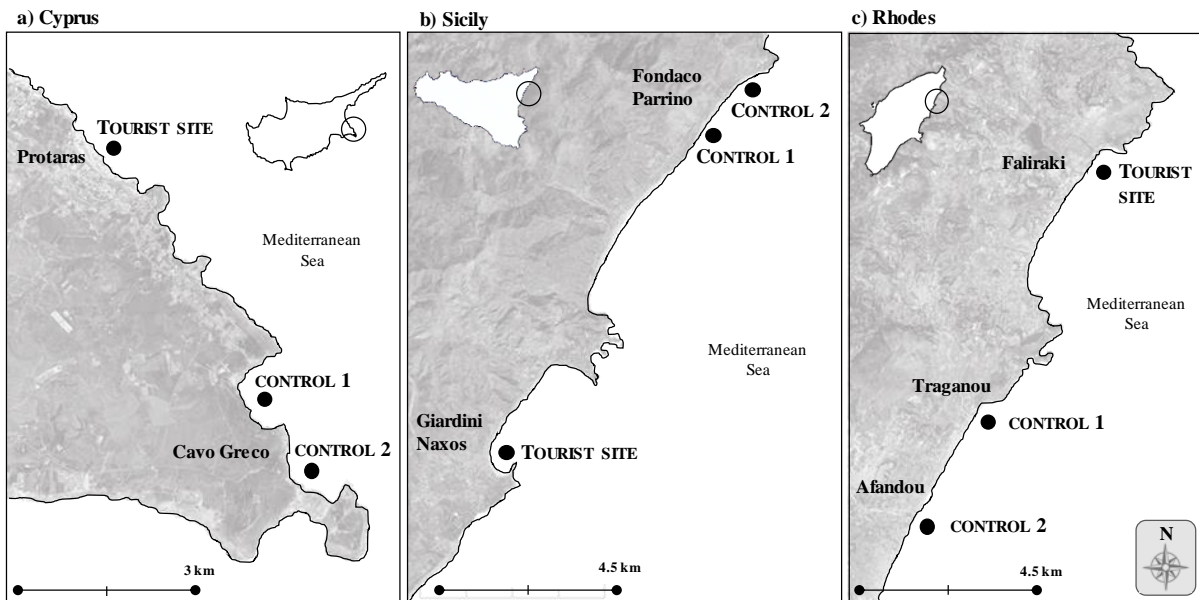
650 Viana, I.G., Bode, A., 2013. Stable nitrogen isotopes in coastal macroalgae: Geographic and  
651 anthropogenic variability. *Sci. Total Environ.* 443, 887–895.  
652 doi:10.1016/j.scitotenv.2012.11.065

653 Vizzini, S., Colombo, F., Costa, V., Mazzola, A., 2011. Contribution of planktonic and benthic  
654 food sources to the diet of the reef-forming vermetid gastropod *Dendropoma petraeum* in  
655 the western Mediterranean. *Estuar. Coast. Shelf Sci.* 96, 262–267.  
656 doi:10.1016/j.ecss.2011.11.021

657 Vizzini, S., Mazzola, A., 2006. The effects of anthropogenic organic matter inputs on stable  
658 carbon and nitrogen isotopes in organisms from different trophic levels in a southern  
659 Mediterranean coastal area. *Sci. Total Environ.* 368, 723–731.  
660 doi:10.1016/j.scitotenv.2006.02.001

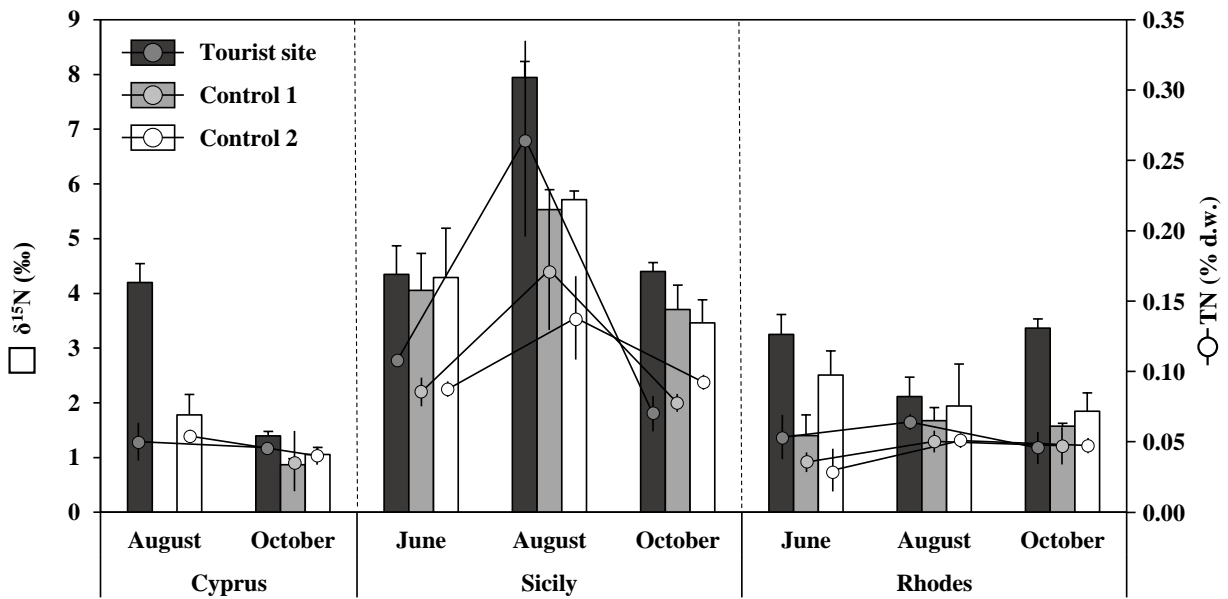
661 Vizzini, S., Mazzola, A., 2004. Stable isotope evidence for the environmental impact of a land-  
662 based fish farm in the western Mediterranean. *Mar. Pollut. Bull.* 49, 61–70.  
663 doi:10.1016/j.marpolbul.2004.01.008

664 Watson, D.F., Philip, G.M., 1985. A refinement of inverse distance weighted interpolation.  
665 *Geoprocessing* 2, 315–327.  
666



670 Fig. 1. Experimental sites in a) Cyprus, b) Sicily (Italy) and c) Rhodes (Greece).

672

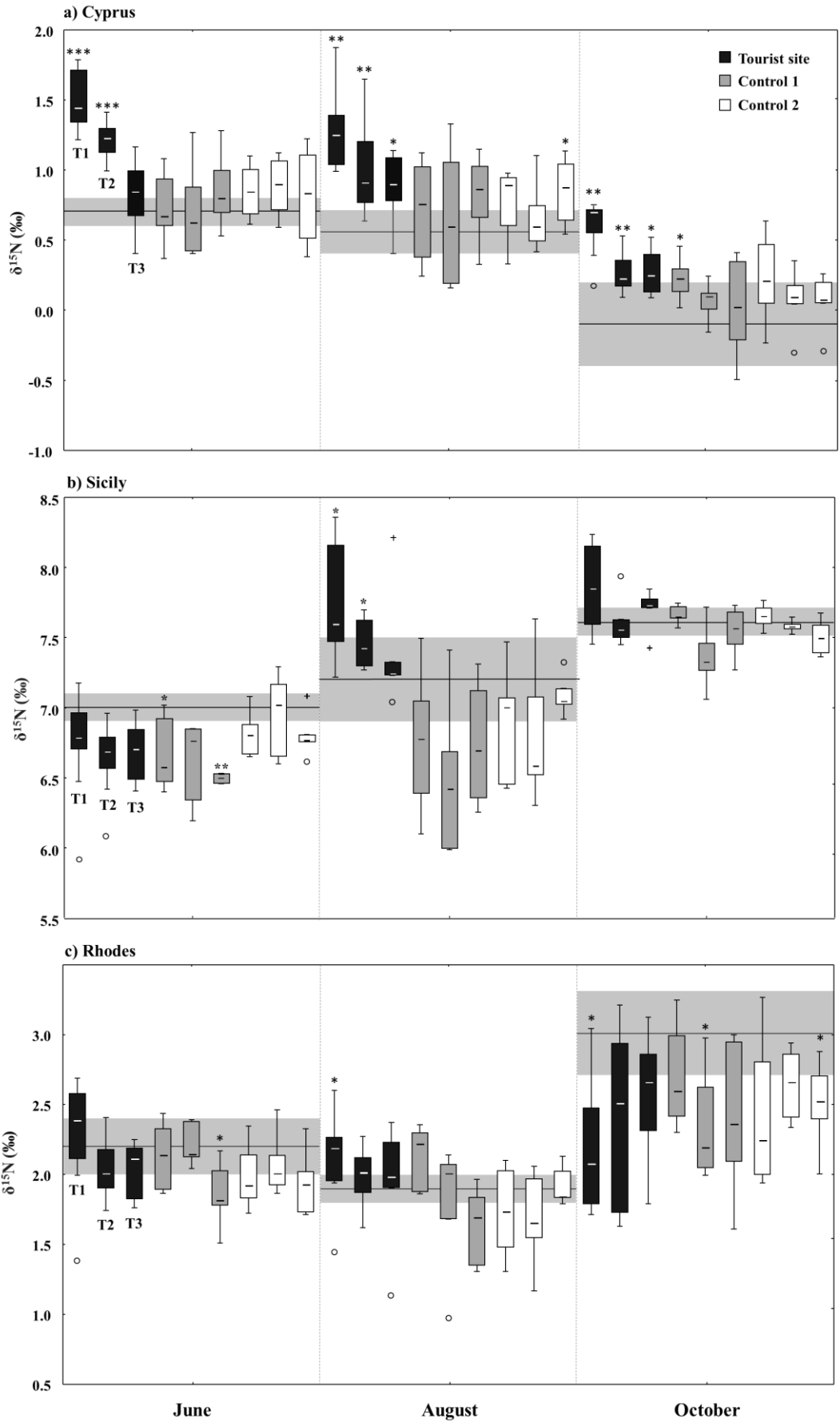


673

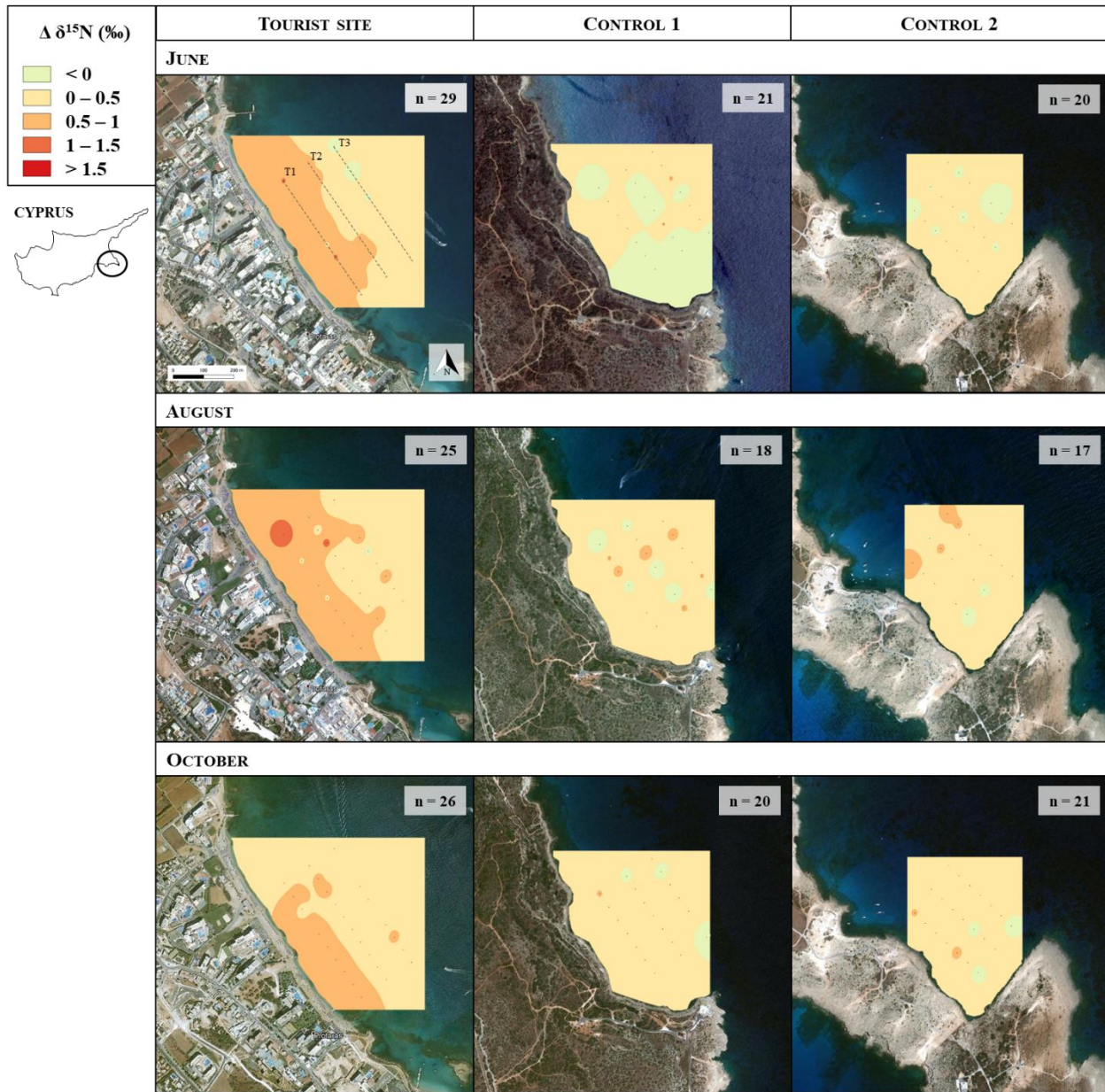
674 Fig. 2. Mean  $\delta^{15}\text{N}$  and TN ( $\pm$  standard deviation, n: 9) of suspended particulate organic matter  
675 (POM) of surface water collected from the three study sites of Cyprus, Sicily and Rhodes in the  
676 different periods (June, August, October). Data from Cyprus in June (all sites) and August (only  
677 Control 1) are lacking because of logistic constraints.

678





680 Fig. 3. Boxplot of  $\delta^{15}\text{N}$  values of the macroalgae deployed along three transects at different  
681 distance from the coastline [T1: 100, T2: 200, T3: 300 m in Cyprus (n: 5-10) and Rhodes (n: 5-  
682 11), T1: 200, T2: 250, T3: 300 m in Sicily (n: 3-12); indicated only below the first three boxes  
683 for the sake of simplicity] in the three study sites (Tourist, Control 1 and 2) in June, August and  
684 October in Cyprus (a), Sicily (b) and Rhodes (c). Each box contains 50% of the data, the thick  
685 horizontal line indicates the median; lower and upper whiskers represent respectively the first  
686 and fourth quartiles of the total range and circles and plus symbols represent respectively outliers  
687 and extremes of the distribution. Asterisks indicate the significance level of the differences  
688 between the  $\delta^{15}\text{N}$  values of the deployed macroalgae and that of the baseline, according to t-test.  
689 p-values: \* = p-value < 0.05, \*\* = p-value < 0.01, \*\*\* = p-value < 0.001. Shadow areas overlaying  
690 the boxplots at each period indicate the mean and the standard deviation of the site and period  
691 specific baseline.  
692



693

694 Fig. 4. Georeferenced maps of  $\Delta\delta^{15}\text{N}$  values in June, August and October 2017 at the Tourist site

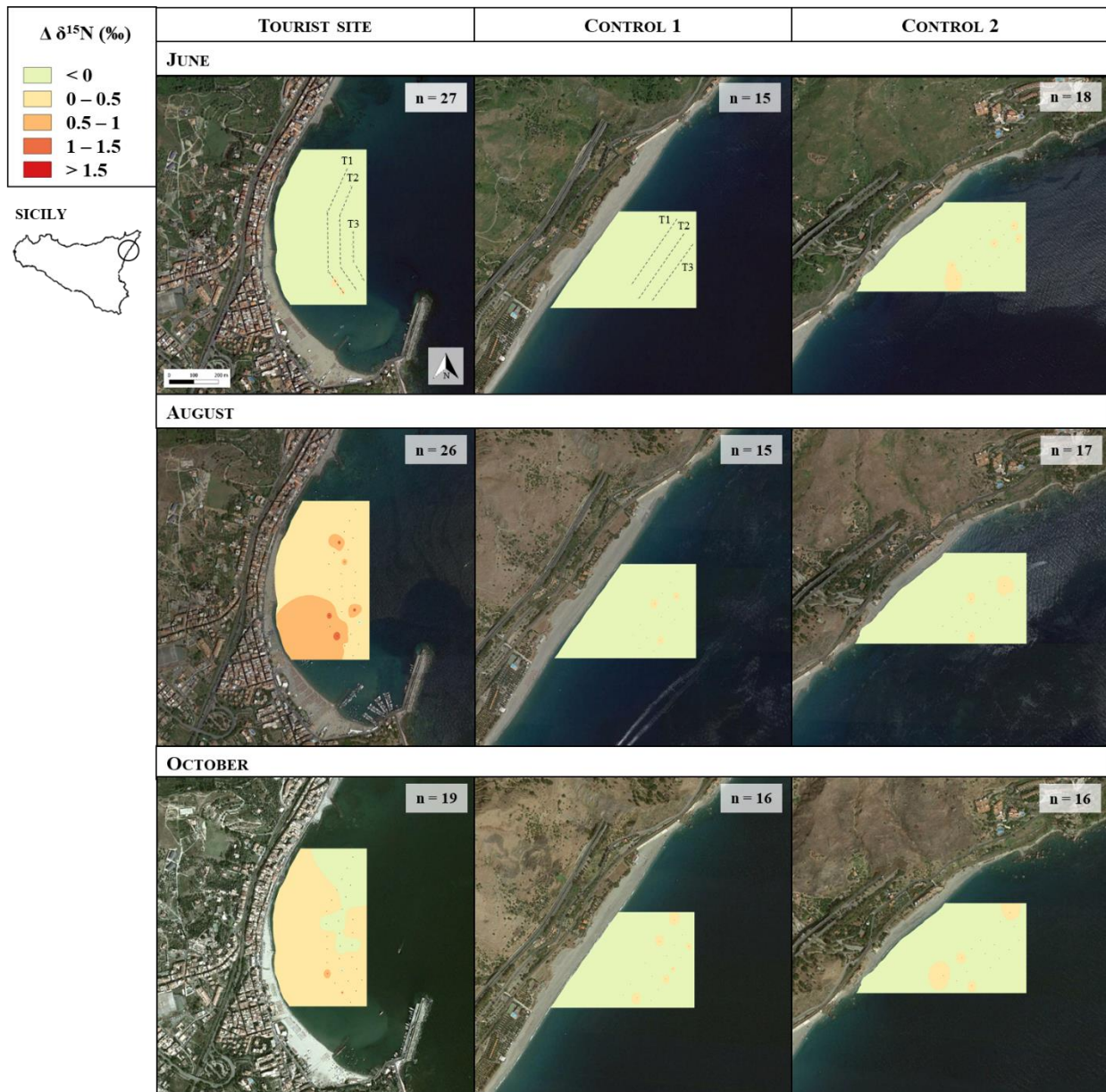
695 and Control sites of Cyprus. Dashed lines (superimposed only to the first panel for the sake of

696 simplicity) indicate the transects at different distance from the coastline (T1: 100, T2: 200 and

697 T3: 300 m) where macroalgae were deployed. The number of the macroalgae deployment

698 devices retrieved at each period and site is also indicated.

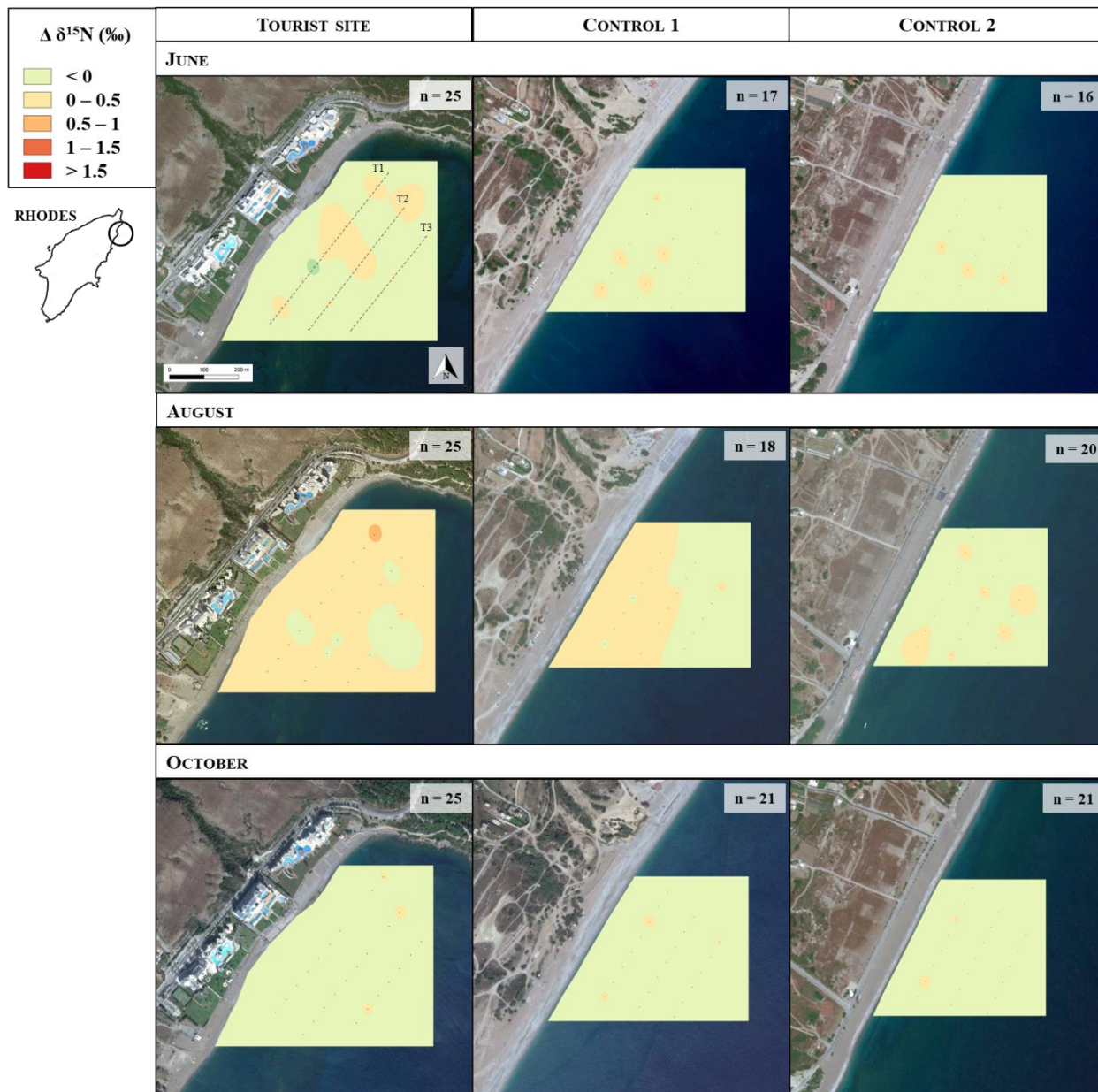
699



700

701 Fig. 5. Georeferenced maps of  $\Delta\delta^{15}\text{N}$  values in June, August and October 2017 at the Tourist site  
 702 and Control sites of Sicily. Dashed lines (superimposed only to the first panel for the sake of  
 703 simplicity) indicate the transects at distance from the coastline (T1: 200, T2: 250 and T3: 300 m)  
 704 where macroalgae were deployed. The number of the macroalgae deployment devices retrieved  
 705 at each period and site is also indicated.

706



707

708 Fig. 6. Georeferenced maps of  $\Delta\delta^{15}\text{N}$  values in June, August and October 2018 at the Tourist site

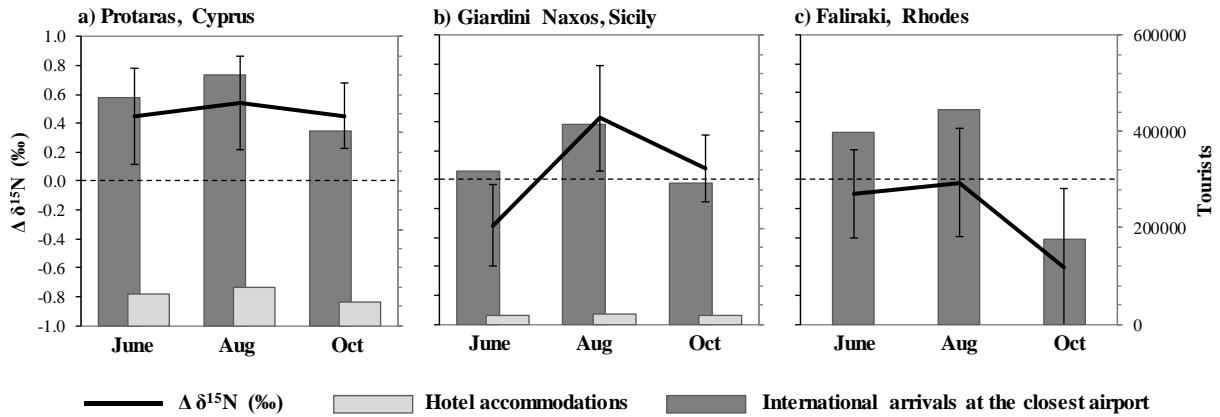
709 and Control sites of Rhodes. Dashed lines (superimposed only to the first panel for the sake of

710 simplicity) indicate the transects at distance from the coastline (T1: 100, T2: 200 and T3: 300 m)

711 where macroalgae were deployed. The number of the macroalgae deployment devices retrieved

712 at each period and site is also indicated.

713



714

715 Fig. 7. Mean  $\Delta\delta^{15}\text{N}$  ( $\pm$  standard deviation, n: 19-29) values recorded in macroalgae deployed at  
 716 the Tourist sites of a) Cyprus (Protaras), b) Sicily (Giardini Naxos) and c) Rhodes (Faliraki) in  
 717 the different periods (June, August, October), superimposed to local hotel accommodations (only  
 718 at Protaras and Giardini Naxos) and International arrivals at the closest airports.

719

720 **Tables**

721

722 Table 1. Mean ( $\pm$  standard deviation, s.d., n: 6), minimum (min) and maximum (max)  
 723 temperature ( $^{\circ}$ C) and salinity (psu) of surface waters in Cyprus, Sicily and Rhodes, in the  
 724 different periods (June, August, October).

Island	Period	T ( $^{\circ}$ C)				S (psu)			
		mean	s.d.	min	max	mean	s.d.	min	max
Cyprus	June	22.4	0.2	21.9	22.9	38.1	0.2	37.5	38.2
	August	29.0	0.2	28.8	29.4	41.2	0.2	41.0	42.0
	October	25.6	0.3	25.0	26.1	40.7	0.8	38.9	41.0
Sicily	June	22.1	0.5	21.3	22.9	38.2	0.6	37.2	38.7
	August	25.9	0.4	25.5	26.7	38.8	0.1	38.7	38.9
	October	22.1	1.1	20.8	24.1	38.4	0.1	38.3	38.6
Rhodes	June	26.2	0.3	25.2	26.9	38.4	0.3	38.1	38.6
	August	30.5	0.8	29.3	32.0	41.5	0.8	41.2	41.8
	October	28.3	0.5	26.9	29.0	40.2	0.5	39.8	40.5

725

726

727 Table 2. Mean values ( $\pm$  standard deviation, s.d., n: 5) of  $\delta^{15}$ N, total N and C/N of the  
 728 macroalgae used as baseline in all islands (Cyprus, Sicily and Rhodes) and periods (June,  
 729 August, October).

Island	Period	$\delta^{15}$ N (‰)		TN (%)		C/N	
		mean	s.d.	mean	s.d.	mean	s.d.
Cyprus	June	0.7	0.1	0.8	0.1	48.7	5.8
	August	0.5	0.2	0.7	0.1	46.4	2.5
	October	-0.1	0.3	0.7	0.1	41.0	4.7
Sicily	June	7.0	0.1	1.0	0.0	34.7	1.9
	August	7.2	0.3	1.3	0.2	26.0	5.9
	October	7.6	0.1	0.8	0.0	34.8	2.0
Rhodes	June	2.2	0.2	0.8	0.1	40.6	4.2
	August	1.9	0.1	0.9	0.1	24.2	1.7
	October	3.0	0.3	1.2	0.2	21.7	2.8

730